ACCOUNTS of chemical research

Article

pubs.acs.org/accounts

Mesoscopic Features of Charge Generation in Organic Semiconductors

Brett M. Savoie, Nicholas E. Jackson, Lin X. Chen,* Tobin J. Marks,* and Mark A. Ratner*

Department of Chemistry, the Materials Research Center, and the Argonne-Northwestern Solar Energy Research Center, Northwestern University, Evanston, Illinois 60208, United States

Supporting Information

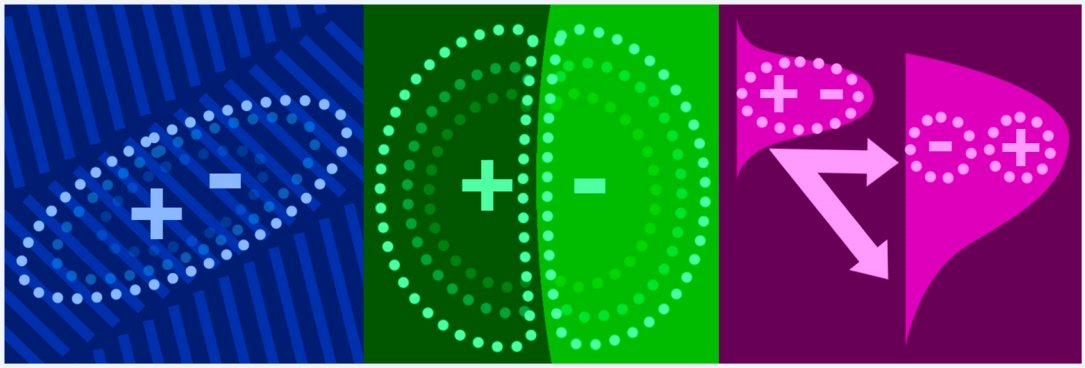

CONSPECTUS: In the past two decades, organic materials have been extensively investigated by numerous research groups worldwide for implementation in organic photovoltaic (OPV) devices. The interest in organic semiconductors is spurred by their potential low cost and facile tunability, making OPV devices a potentially disruptive technology. To study OPV operating mechanisms is also to explore a knowledge gap in our general understanding of materials, because both the time scales (femtosecond to microsecond) and length scales (nanometer to micrometer) relevant to OPV functionality occupy a challenging and fascinating space between the traditional regimes of quantum chemistry and solid-state physics.

New theoretical frameworks and computational tools are needed to bridge the aforementioned length and time scales, and they must satisfy the criteria of computational tractability for systems involving 10^4−10^6 atoms, while also maintaining predictive utility. While this challenge is far from solved, advances in density functional theory (DFT) have allowed researchers to investigate the ground- and excited-state properties of many intermediate sized systems (10^2−10^3 atoms) that provide the outlines of the larger problem. Results on these smaller systems are already sufficient to predict optical gaps and trends in valence band energies, correct erroneous interpretations of experimental data, and develop models for charge generation and transport in OPV devices.

The active films of high-efficiency OPV devices are comprised of mesoscopic mixtures of electron donor (D) and electron acceptor (A) species, a "bulk-heterojunction" (BHJ) device, subject to variable degrees of structural disorder. Depending on the degree of intermolecular electronic coupling and energy level alignment, the spatial delocalization of photoexcitations and charge carriers can affect the dynamics of the solar cell. In this Account, we provide an overview of three pivotal characteristics of solar cells that possess strong delocalization dependence: (1) the exciton binding energy, (2) charge transfer at the D−A heterojunction, and (3) the energy landscape in the vicinity of the D−A heterojunction. In each case, the length scale dependence can be assessed through DFT calculations on reference systems, with a view to establishing general trends. Throughout the discussion, we draw from the experimental and theoretical literature to provide a consistent view of what is known about these properties in actual BHJ blends. A consistent interpretation of the results to date affords the following view: transient delocalization effects and resonant charge transfer at the heterojunction are capable of funneling excitations away from trap states and mediating exciton dissociation; these factors alone are capable of explaining the remarkably good charge generation currently achieved in OPV devices. The exciton binding energy likely plays a minimal role in modern OPV devices, since the presence of the heterojunction serves to bypass the costly exciton-to-free-charge transition state.

INTRODUCTION

Photovoltaic devices operate by converting individual photoexcitations into electrons and holes, which are then collected in an external circuit.[1] The challenge for all photovoltaic technologies is to effect this conversion while minimizing losses associated with incomplete light absorption, charge carrier relaxation, and recombination.[2] In organic photovoltaics (OPVs), an additional challenge is introduced by the fact that the primary

Special Issue: DFT Elucidation of Materials Properties

Received: February 26, 2014
Published: July 22, 2014

   dx.doi.org/10.1021/ar5000852 | Acc. Chem. Res. 2014, 47, 3385−3394

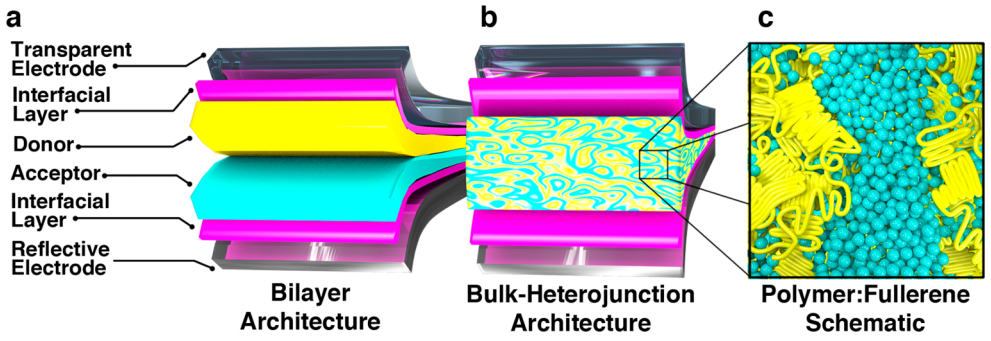

Figure 1. Organic photovoltaic device schematics. (a) Bilayer device configuration. Donor and acceptor layers are deposited separately, resulting in minimal interfacial area and suppressed photocurrent. (b) Bulk-heterojunction (BHJ) device configuration. Donor and acceptor species are co-deposited, distributing the heterojunction throughout the active layer. (c) Schematic depiction of a polymer/fullerene BHJ. Regions of high polymer order exist alongside disordered and mixed domains. Domain thicknesses are inhomogeneous, although the highest performing devices maintain enough phase separation to achieve long-lived charge generation and collection.

photoexcited species in organic semiconductors are not spatially separated electron−hole pairs but instead bound short-lived species called excitons. In its most common usage, the appellation "excitonic" simply refers to any system whose lowest photoexcited state is marked by a high degree of electron−hole correlation, meaning that the electron and hole occupy a similar region of space and that the energy required to separate them into noninteracting electrons and holes exceeds the available thermal energy.

The distinguishing mechanistic feature of excitonic photovoltaics is that some secondary process, following the photoexcitation, is required to efficiently break up the exciton and generate collectable charge. In 1958, Kearns and Calvin demonstrated that charge generation could be facilitated by utilizing two laminated organic semiconductor films, one with high hole affinity (electron donor) and one with high electron affinity (electron acceptor).[3] When the ionization potential of the donor, electron affinity of the acceptor, and optical bandgaps of the two materials are appropriately tuned, the bound photoexcitations in each phase can dissociate into charge carriers at the interface between the two materials. To this day, state-of-the-art OPVs are designed according to the same donor−acceptor principle originally described by Kearns and Calvin.

Major OPV advances have been achieved since 1958. The bilayer concept (Figure 1a) remained dormant until being substantially refined by Tang, whose report of a device with ∼1% solar power conversion efficiency (PCE) in 1984 validated the concept.[4] Later, Yu and co-workers discovered that efficient BHJ blended film morphologies can be obtained by simple co-deposition of the donor and acceptor (Figure 1b).[5] The BHJ concept realigned the field by boosting PCEs and further lowering fabrication costs. The complex interpenetrating BHJ structure (Figure 1c) also spawned a vast film processing literature, the fruit of which is the mélange of processing methodologies now routinely used in device fabrication. Over the same period, polymers became widely used as donors due to their excellent solution proccessability and superior rheological properties versus molecular semiconductors (a trend that has been partially reversed in recent years), and fullerene derivatives were ubiquitously adopted as OPV electron acceptors (a trend that has not been substantially reversed). The most recent realignment occurred with the near-universal shift from homopolymers and small molecules to low-bandgap copolymers and in-chain donor−acceptor chromophores.[6]

Through all of these developments, the basic operating principles of OPVs have remained simple in outline: light absorption leads to exciton formation, the excitons dissociate at a heterojunction between a donor and an acceptor, and the phase-separated charges are collected. Although this is an attractively simple outline, we have only lately developed the tools necessary to investigate the quantum details of these processes. These are large problems, both in terms of the number of atoms involved (e.g., typical OPV repeat units possess ∼100 atoms) and the irreducible complexity of dealing with structurally disordered systems. The quantum details and chemical descriptors are still lacking that are necessary to address key questions: (i) What is the exciton binding energy and can it be synthetically tuned? (ii) What quantum states mediate exciton dissociation processes? (iii) What is the energy landscape in the vicinity of the heterojunction?

To date, many different high-PCE polymer/fullerene BHJ blends have been structurally and spectroscopically interrogated, affording a fairly complete and surprisingly general description of the device photodynamics (Figure 2).[7−12] Depending on the details of phase segregation, most or all of the photoexcitations in BHJ-OPVs undergo charge transfer in <100 fs.[10] Those that do not, typically a minority, undergo slower diffusive motion until they find a site for charge transfer on the 1−100 ps time scale.[10,11] There is generally no differential charge generation efficiency for excitons dissociated on the two time scales.[10,11] Following charge transfer, the potential exists for the electron and hole to remain electrostatically bound across the heterojunction, resulting in the formation of a charge-transfer (CT) state (other terminologies exist, with this the most common.)[7,8] In some blends, CT states seem to play a minimal role; in others, geminate recombination via CT states represents the largest loss channel.[7] CT states carry several distinguishing features: they can be both temporally and energetically resolved from the donor and acceptor excitonic states using spectroscopy,[8,11,13] their recombination dynamics are monomolecular,[7] and they act predominantly as a loss channel[7,8,12] (i.e., excitons in high-performing blends do not first form CT states that later thermally dissociate into free charges). For those photoexcitations that bypass relaxed CT states and form separated electrons and holes, collection takes place via charge migration within the donor and acceptor phases. The time scale for "sweep out" (i.e., the time required for charge to exit the device) is variously placed on the 10^{-7}−10^{-4} s time scale.[14] Depending on the device details and operating voltage, carrier transport may be dominated by either diffusion or drift.[15]

dx.doi.org/10.1021/ar5000852 | Acc. Chem. Res. 2014, 47, 3385−3394

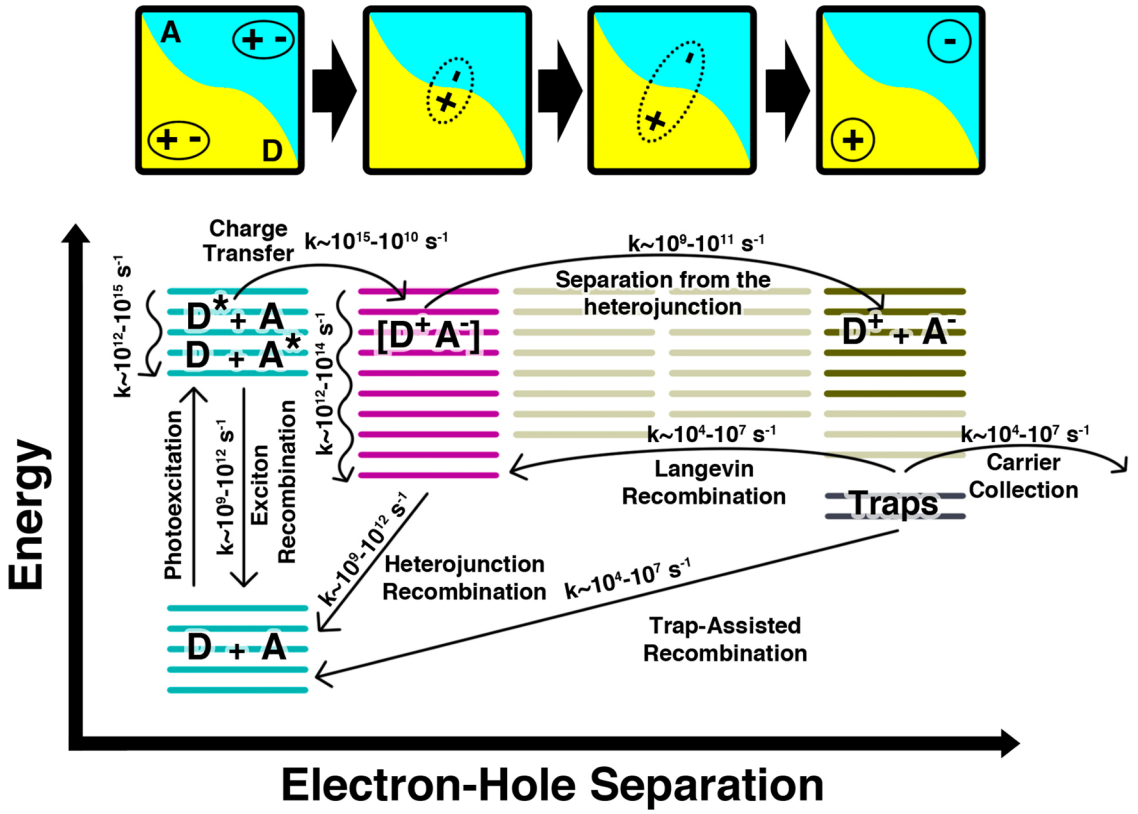

Figure 2. State manifolds and time scales relevant to organic photovoltaic action. Wavy arrows depict relaxation processes (e.g., thermalization and polaron formation). Ground state (D + A) and excitonic (D* + A, D + A*) manifolds are labeled teal, charge-transfer (CT) states ($[D^+A^-]$) are labeled pink, intermediate and fully separated polaron states ($D^+ + A^-$) are labeled gold, and traps are labeled gray. Rates are collated from representative publications and apply to standard operation light intensities (see Supporting Information for an extended bibliography). Triplet dynamics have been neglected, for the sake of clarity. Schematic depictions of the primary generation processes are above.

THE EXCITON BINDING ENERGY

Exciton characteristics, including spatial extent and binding energy, vary depending on the identity of the light absorbing unit(s) and the excitation spin state. In general, triplet states are lower in energy and more localized than singlet states due to the symmetry properties of triplet wave functions,[16] and singlet states are the primary charge precursor in most OPVs.

The binding energy of singlet excitons, E_B, is a commonly referenced quantity in OPVs, because the energetic cost associated with dissociating this species ultimately subtracts from the achievable device voltage. E_B is also a property that can potentially be screened for individual donors to expedite time-consuming OPV blend optimization.[17] E_B has a simple chemical definition in terms of the free energy associated with the following photoionization reaction:

$$M + M^* \xrightarrow{E_B} M^+ + M^- \quad (1)$$

where M is a generic chromophore in its ground state, M* is the relevant photoexcited state, and M^+ and M^- are the cationic and anionic species, respectively. The formation energies of each species can be independently measured as the optical bandgap ($E_{g,opt}$), the ionization potential (IP), and the electron affinity (EA),

$$M \xrightarrow{E_{g,opt}} M^* \quad (2)$$

$$M \xrightarrow{IP} M^+ \quad (3)$$

$$M \xrightarrow{-EA} M^- \quad (4)$$

yielding the following beguilingly simple definition for the binding energy:

$$E_B = E_{g,T} - E_{g,opt} \quad (5)$$

The IP − EA difference has been relabeled as $E_{g,T}$, reflecting its common reference as the "transport" gap ("electrochemical" gap or "fundamental" gap are also used.)

While eq 5 is a straightforward thermodynamic definition of E_B, evaluation of the relevant ionization potentials, electron affinities, and optical transitions necessary to determine meaningful E_B values is nontrivial.[18] All of the ingredients in eq 5 are obviously affected, for instance, by whether M is in vacuum or embedded in a matrix. Similarly, in disordered films, which are the most technologically relevant environment for defining E_B, these energies are broadened by structural and conformational disorder,[19] intermolecular couplings,[20] and local dielectric environment,[21] which make the binding energy a function of the local exciton environment. The combination of these mechanisms results in shifts between vacuum, solution, and film measurements of these energies (Figure 3).

E_B is also a dynamical property, due to the time-dependence of the relaxation processes that follow photoexcitation and charge formation. For example, the charge-density redistribution following photoexcitation engenders electronic and nuclear relaxation processes that stabilize the excited state (the Stokes shift) while at the same time increasing E_B. In contrast, long-time scale (greater than picosecond) structural and electronic relaxation of

dx.doi.org/10.1021/ar5000852 | Acc. Chem. Res. 2014, 47, 3385−3394

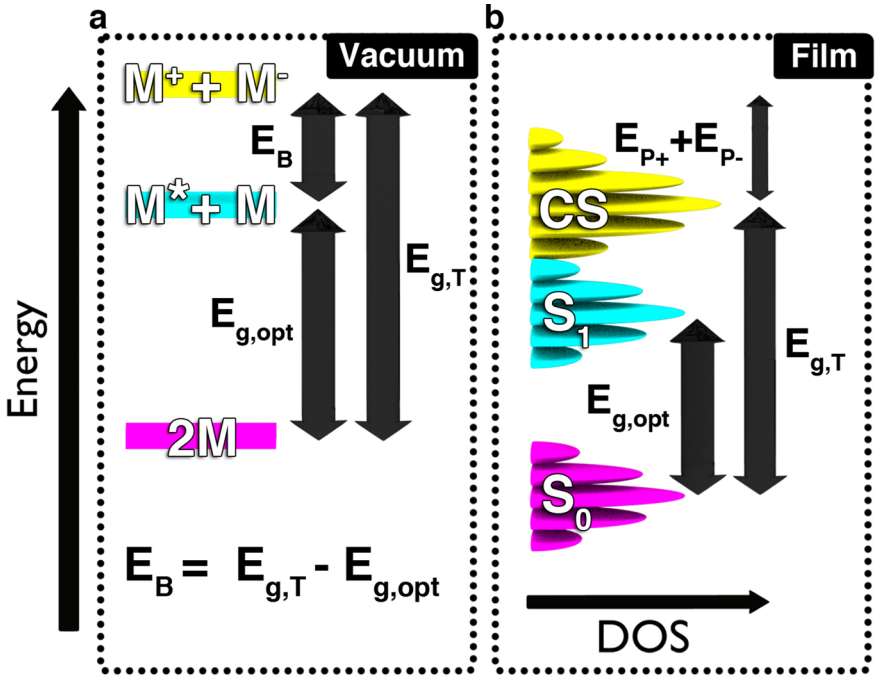

Figure 3. Energy shifts associated with vacuum and film measurements. (a) In vacuum, well-defined discrete states and bandgaps exist. $E_{g,opt}$ is generally lower in energy than the $E_{g,T}$ due to the electron-hole stabilization of the former. (b) In films, a combination of structural inhomogeneity and intermolecular coupling broaden discrete molecular states into state manifolds (S_0, S_1, CS). All states are lowered in energy due to the higher dielectric constant of the condensed phase, although the individual bandgaps may blue or red-shifted. In general, ionic states are strongly stabilized by the structural and electronic relaxation of neighboring molecules (polaron formation). E_{P+} and E_{P-} are the polaronic stabilization of the cation and anion species, respectively.

the cation and anion species (polaron formation) reduces E_B by stabilizing the species on the right-hand side of eq 1. The lower limit for E_B is obtained by taking the unrelaxed vertical excited state (diabatic) as the reference excitation, and the fully relaxed (adiabatic) anion and cation polarons as the reference charge separated state. Physically, this would be the energy associated with ionizing the excited state prior to any relaxation processes (Figure 4a).

Modern DFT software makes it straightforward to calculate the optical and transport gaps of common organic donors, although what was said with regard to experimental measurements of $E_{g,T}$ and $E_{g,opt}$ also applies to the computational methodologies: *getting a number is easy, but ensuring the physicality is more difficult*. For example, within the TDDFT formalism, excitation energies are highly sensitive to the long-range exchange incorporated into the functional, with local density (LDA) and generalized gradient approximated (GGA) functionals failing to produce bound excited states.[22] On the other hand, while popular hybrid functionals (e.g., B3LYP) include a variable amount of long-range Hartree−Fock exchange and produce bound excitations, E_B becomes a function of the amount of exchange chosen to be incorporated into the functional.[23] Hybrid functionals also fail to reproduce the correct long-range exchange and correlation behaviors, resulting in hybrid TDDFT calculations generally underestimating the energy of the charge-transfer photoexcitations germane to OPV donors (e.g., PTB7 and PCPDTBT in Figure 4b).[24] Range-separated functionals (e.g., cam-B3LYP, ωB97X, OT-BNL) provide a convenient solution to the shortcomings of hybrid functionals by stitching together separate, independently accurate, short-range and long-range functionals.[25] The remaining difficulty is to remove artifacts associated with the choice of range-separation parameters. An optimal-tuning algorithm recently developed by Stein et al. resolves this dilemma by self-consistently tuning the range-separation parameter from calculation to calculation to maximize the fidelity between the frontier Kohn−Sham eigenvalues and the predictions of Koopmans' theorem.[24] This physically motivated tuning criterion has proven to be remarkably robust for predicting the optical gap of systems of both varying size and varying charge-transfer character.

Figure 4c shows optimally tuned (OT) calculations of E_B for four heavily investigated OPV polymers in vacuum, including the oligomer length dependence. Here the anion, cation, and neutral oligomer geometries are optimized using EDF1/6-31G* (a semi-empirical GGA functional and moderate basis set); then single-point DFT and TDDFT OT-BNL/6-311G** calculations are performed to obtain the cation, anion, and neutral total energies and excited state spectra. $E_{g,T}$ (adiabatic) was determined on the basis of total energy differences of the geometry optimized anion and cation species, and $E_{g,opt}$ (diabatic) was determined from the lowest singlet excitation in the TDDFT calculation on the neutral species.

It has been speculated that copolymers possessing donor−acceptor interactions may form destabilized excitons that facilitate charge generation.[26,27] The calculations shown in Figure 4c suggest that the copolymers possess modestly suppressed E_B values relative to homopolymers of similar conjugation length. This difference is attributable to a combination of increased planarity, which engenders a greater effective conjugation length, and higher electron affinity (EA), which lowers the energetic cost of forming the anion from the excited state. Variable E_B effects may explain the differential photodynamics observed across series of polymers possessing similar constitution and morphological character.[28]

Another interpretation of the data in Figure 4c is that the strong conjugation length dependence of E_B implies that

dx.doi.org/10.1021/ar5000852 | Acc. Chem. Res. 2014, 47, 3385−3394

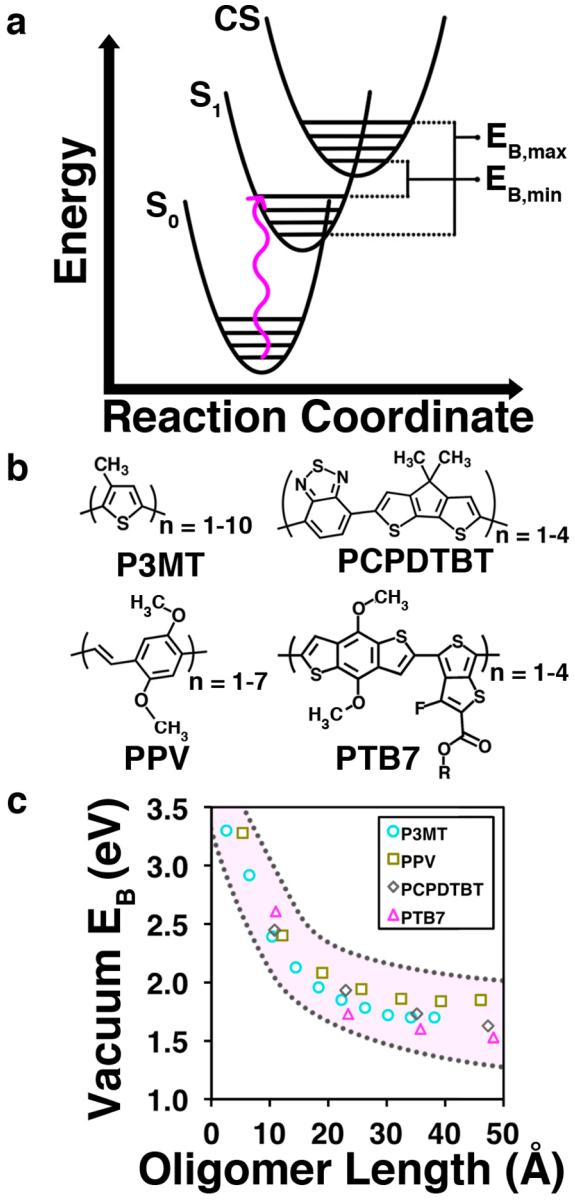

Figure 4. (a) In the Franck–Condon picture, each parabola represents an electronic state and lines represent vibrational states. Since the ground and excited state relaxed geometries are not congruent, vertical excitation is followed by thermalization via internal and external nuclear reorganization; similarly, charge separation is accompanied by additional (possibly orthogonal) relaxations. (b) Chemical structures of the studied materials. (c) The vacuum E_B length dependence for two common homopolymers (P3MT and PPV) and two common copolymers (PCPDTBT and PTB7). No external contributions (polaron formation) to the binding energy are considered here, which makes these values much larger than the corresponding film values. The pink band is drawn as a guide to the eye.

polymer ordering effects, such as would affect the distribution of conjugation lengths within the film, are capable of overwhelming intrinsic effects associated with the repeat units of copolymers versus those of homopolymers. Convincing evidence for this comes from pump–probe experiments quantifying the yield of free charge from direct photoexcitation of pristine polymers (no acceptor). Elegant demonstrations for P3HT show that the charge yield can be tuned by controlling the regioregularity, molecular weight, or microstructure while otherwise keeping the repeat unit constant.[17,27] While the experimental picture for copolymers is less complete, intrinsic effects associated with E_B lowering in copolymers appear to be slight. For example, Tautze et al. reported a comparison of the quantum yield (QY) of photogenerated charge for pristine P3HT (a homopolymer) and several copolymers, finding that their best copolymer (a material related to PCPDTBT in Figure 4b) exhibited a 2-fold increase in QY over P3HT.[26] In the same study, P3HT facilitates the longest-lived charge generation, and the authors offered no controls for morphological differences between samples. Using microwave spectroscopy, Reid et al. reported the opposite result, finding that on the nanosecond time scale, pristine P3HT produces twice the long-lived charge of another prominent copolymer, PCDTBT.[27] Similarly, Vardeny reported a QY ≈ 30% in P3HT films, which appears to be greater than any report for copolymers to date.[17]

The experimental results on charge generation in pristine films suggest a more subtle view of the relationship between E_B, morphology, and charge generation. In an inhomogeneous film, it is not necessary (or likely) that the photoexcitation will occur on a segment with the same conjugation length as the eventual host of the cation and anion polarons. Photoexcitations originating on short segments might ionize onto long segments, and vise versa (Figures 5a,b). By combination of length-dependent calculations of $E_{g,T}$ and $E_{g,opt}$ with COSMO calculations to estimate the polaron energy of films (E_{P+} and E_{P-} in Figure 3b), the E_B values associated with various combinations of photoexcitation and polaron conjugation length can be evaluated.

Figure 5c shows the results of a length dependent E_B analysis for P3MT. E_B values along the diagonal, ranging from 0.1 to 0.4 eV, are typical of conjugated polymers.[29] The off-axis components of Figure 5c represent dissociation energies when the excitation and polarons are located on different length conjugated segments. The results show that variable conjugation length segments, of ostensibly the same material, are capable of exothermic charge generation. The explanation is straightforward: short segments host high-energy excited states, whereas long segments host stable polaron states. It seems plausible that in structurally disordered films, exciton breakup is actually "catalyzed" by heterojunctions between long and short conjugated segments of polymer, such as would occur at backbone kinks and interchain crossings generated by conformational disorder. The cooperation of both factors also explains the counterintuitive observation that *homogeneous* pristine films actually suppress free charge generation;[27] some variation within the film conjugation lengths is apparently required for efficient charge generation.

■ CHARGE GENERATION IN OPVS

Are Copolymers Different?

While comparisons across pristine film studies are difficult due to insufficient controls for excitation intensity,[30] morphology,[27] doping,[31] and spectral assignment,[17] a consistent synthesis of the spectroscopic and computational literature seems incompatible with the proposition that copolymers are distinguished from homopolymers by an enhanced ability to dissociate excitons.

Yet, even if copolymer excitons do not generally exhibit an enhanced propensity for charge generation in pristine films, it is still possible that they possess an advantage for OPV charge generation. It is thus instructive to compare the charge generation of pristine materials to their corresponding charge generation in optimized OPV devices as measured by the internal quantum efficiency (IQE), the number of charges collected divided by the number of photons *absorbed*. For instance, the

dx.doi.org/10.1021/ar5000852 | Acc. Chem. Res. 2014, 47, 3385–3394

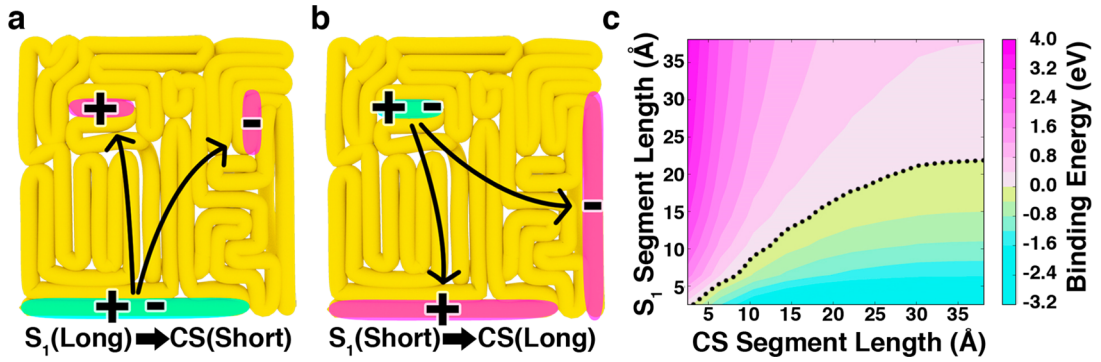

Figure 5. Schematic depiction of exciton dissociation between photoexcited and charge separated segments of different length. (a,b) Photoexcitation on a long (short) segment leads to delocalized polarons on short (long) segments. (c) A two-dimensional plot of E_B, for different combinations of conjugation length P3MT segments hosting the photoexcitation and charge separated state, with COSMO solvation energies ($\varepsilon_r = 4$) added to diabatic $E_{g,T}$ values.

copolymer PCDTBT only produces about half the long-lived charge of pristine P3HT in THz experiments,[27] yet when blended with fullerene it is capable of >90% IQE.[32] This remarkable metric surely means that this material combination has no difficulty separating excitons. On the other hand, seven years prior, Schilinsky et al. reported >90% IQE for P3HT blended with fullerene, using similar characterizations.[33] It has also been shown that excitons originating on OPV acceptors can dissociate with equal efficiency compared with excitons originating on donor copolymers or homopolymers,[34] which also undermines the hypothesis that donor excitons, in general, are special charge precursors in OPVs.

While the results for OPV quantum efficiencies are in tension with the idea that weakly bound copolymer excitons are critical for high-performing blends, there are several unique properties of copolymers that are certainly advantageous. Copolymers generally have better absorption overlap with the solar spectrum, which increases their potential current production. In general, copolymers also have tunable energetics for maximizing device voltages. There is also evidence that copolymers form advantageous morphologies with fullerenes that are distinct from the morphologies of highly crystalline homopolymers like P3HT.[28] These factors alone seem capable of explaining most of the superior efficiencies reported in the literature without appealing to special properties of copolymer excitons.

Exciton Delocalization in OPVs

Figure 4c shows that E_B is a sensitive function of the conjugation length of the polymer, with delocalization generating more weakly bound excitons. Several groups have also speculated on the connection between the rapid time scale of charge-transfer in OPVs (<100 fs for most excitations) and charge generation efficiency, on the basis that a newly formed exciton is less strongly bound than a long-lived exciton.[10] Unfortunately, most evidence to date contradicts the view that unrelaxed excitations are privileged precursors to free charge. Heeger's group recently published a conclusive illustration of this, showing that for three donor/acceptor blends with >90% device IQE, 40% of excitons dissociate on a diffusion-limited time scale (100−1000 ps).[10] The only way to reconcile those two numbers (>90% IQE and 40% diffusion-limited) is to conclude that there is no differential outcome for excitons dissociated on the ultrafast and diffusion-limited time scales.[35]

One mechanism through which delocalization can aid dissociation, independent of ultrafast arguments, is by decoupling excitonic states from localized CT states at the heterojunction

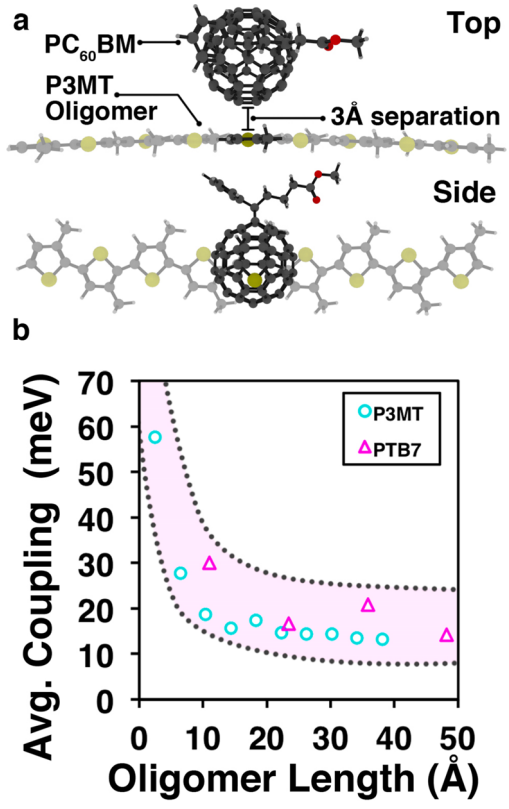

Figure 6. Delocalization dependence of the donor−acceptor coupling. (a) A depiction of the coupling geometries. (b) The average LUMO/LUMO, LUMO/LUMO + 1, and LUMO/LUMO + 2 donor/acceptor couplings calculated at the DZP/B3LYP level of theory for P3MT and PTB7 oligomers aligned along the $PC_{60}BM$ acceptor. The pink band is drawn as a guide to the eye.

(Figure 2). Localization of the electron and hole on neighboring molecules maximizes the electron−hole Coulombic interaction, making the lowest energy CT states also the most localized.[12] Since the electronic coupling is proportional to the wave function overlap, as the photoexcitation delocalizes, it decouples from any single fullerene, concomitantly also decoupling from the lowest energy CT states. We have demonstrated this mechanism for model P3MT/$PC_{60}BM$ and PTB7/$PC_{60}BM$ heterojunctions by varying the size of the donor oligomers while calculating the coupling between the donor and acceptor unoccupied orbitals using the B3LYP Hamiltonian (Figure 6b). Naturally, this

dx.doi.org/10.1021/ar5000852 | Acc. Chem. Res. 2014, 47, 3385−3394

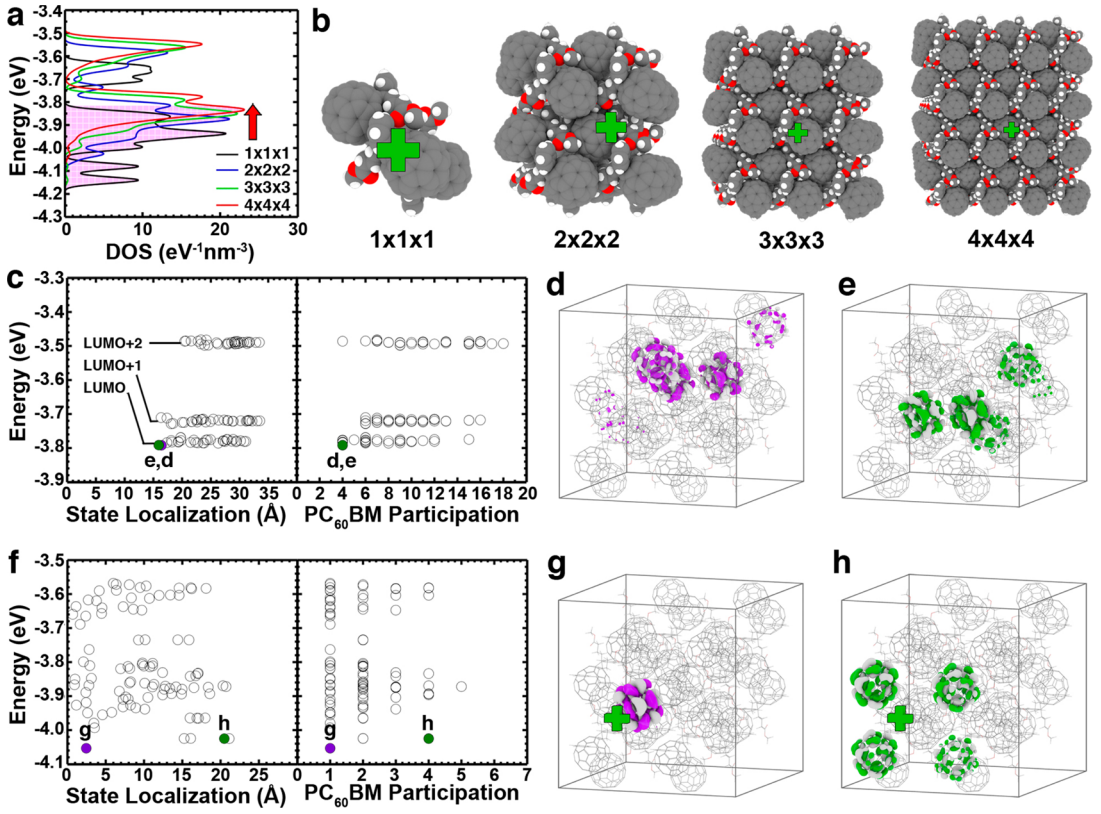

Figure 7. Density of states calculations (DOS) on $PC_{60}BM$ crystallites of varying size, showing the influence of nearby charge on CT state formation. (a) DOS as a function of crystallite size. A point charge positioned ∼3 Å normal to the 001 face is included in each calculation. (b) Images of the geometries sampled in panel a. Localization of the 2 × 2 × 2 crystallite eigenfunctions and the number of molecules contributing to each eigenfunction in the presence (f) and absence (c) of a positive point charge. Visualization of the lowest and second lowest eigenfunctions in the presence (g, h) and absence (d, e) of a positive point charge. Reprinted with permission from ref 12. Copyright 2014 American Chemical Society.

procedure neglects the geometric rearrangements likely occurring at the heterojunction, but the aim is simply to demonstrate the qualitative decoupling behavior as a function of the donor delocalization length. By analogy, a similar mechanism could also slow the recombination rate and destabilize the lowest-energy CT states at heterojunctions between well-conjugated units.

Unequal Donor and Acceptor Participation in Exciton Dissociation

As remarked in the Introduction, the features of successful charge generation in fullerene-based OPVs are remarkably general: CT mediated (geminate) recombination is suppressed,[7,12] the early charge transfer dynamics are independent of both the temperature[9] and the electric field,[12] and these properties are typically reversed when fullerene is replaced with another acceptor.[7] Other general features include the following: charge generation is equally efficient on the ultrafast and diffusion-limited time scales,[10,11] and charge yield is a sensitive function of fullerene concentration and donor−acceptor phase separation.[11,12]

We have suggested[12] that these features can be self-consistently explained by considering the dependence of the energy distribution and localization of CT and CS states on the number and ordering of fullerenes near the heterojunction. DFT calculations were used to parametrize a model Hamiltonian of coupled $PC_{60}BM$ (the most common OPV fullerene derivative) MOs that includes the influence of structural disorder and nearby charge distributions. This approach allows us to investigate clusters of up to 500 fullerenes while accounting for finite-size effects, disorder, and electron−hole interactions.

Fullerenes uniquely possess a 3-fold degenerate LUMO. Although functionalization breaks this degeneracy, all three orbitals remain sufficiently low-lying to participate in charge generation (e.g., the LUMO + 2 and LUMO are separated by ∼0.4 eV in $PC_{60}BM$).[36] This state near-degeneracy leads to several distinguishing features associated with fullerene clusters. For example, the orientational dependencies of the coupling between the different fullerene orbitals are complementary, rendering the average electronic coupling between fullerenes essentially isotropic (∼7 meV over the explored conformational space) and comparable to the internal reorganization energy of $PC_{60}BM$ (∼15 meV at the B3LYP/6-311++G** level).[12] In turn, facile pairwise coupling leads to high electrical connectivity within the fullerene phase that is robust to structural disorder. In our calculations, this is evident as broadly delocalized CS states (Figure 7) that persist under various types of disorder (Figure 8). Moving forward, it will be critical to quantify the time scale and factors that govern localization, foremost by quantifying the electron−phonon coupling in disordered clusters.

Orbital degeneracy also provides a mechanism for bypassing the lowest energy CT states during exciton dissociation. Considering the influence of proximate charge distributions on the electronic structure of $PC_{60}BM$ clusters, we consistently observe that one of the three states is stabilized more strongly than the other two (See Figure 9 for general discussion). In clusters this results in an unbound channel (i.e., an electronically "hot" channel, rather than a vibrationally "hot" channel) for dissociation that persists even in the presence of a nearby hole.

dx.doi.org/10.1021/ar5000852 | Acc. Chem. Res. 2014, 47, 3385−3394

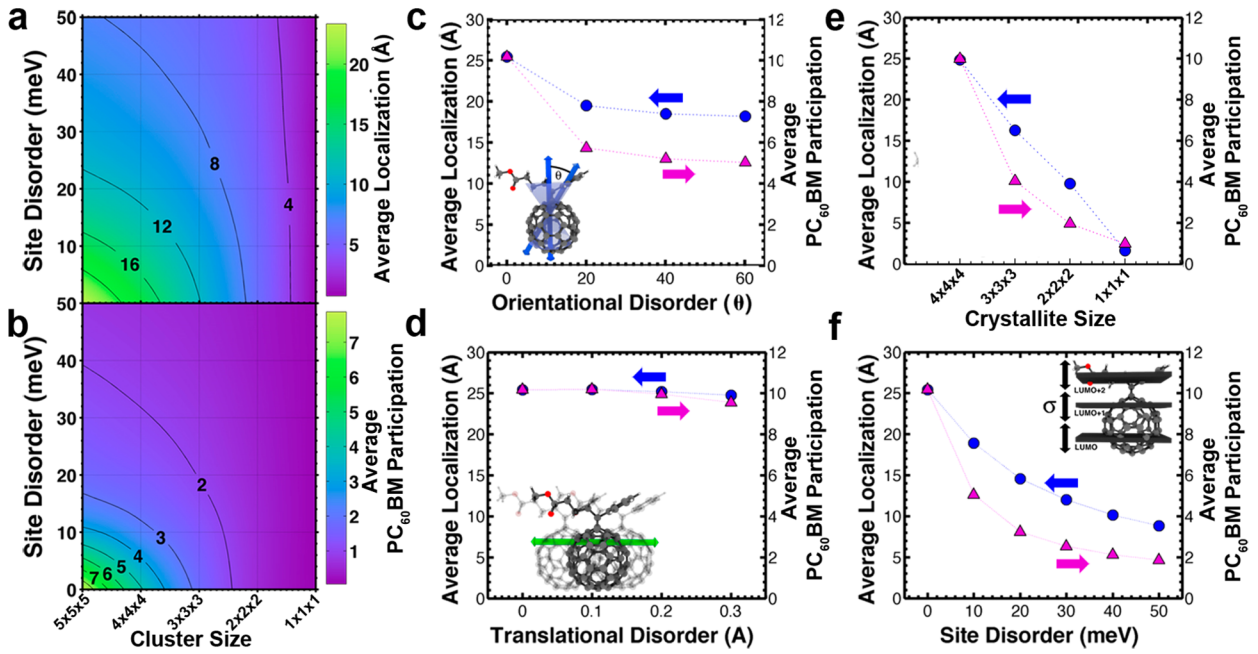

Figure 8. Effect of disorder on the localization and $PC_{60}BM$ participation in the CS states. (a) The average localization and (b) $PC_{60}BM$ participation as a function of cluster size and site disorder. The individual effects of (c) orientational disorder, (d) translational disorder, (e) crystallite size, and (f) site disorder on the average localization and $PC_{60}BM$ participation. Each data point in all plots (a–f) is averaged over 100 simulated clusters. Reprinted with permission from ref 12. Copyright 2014 American Chemical Society.

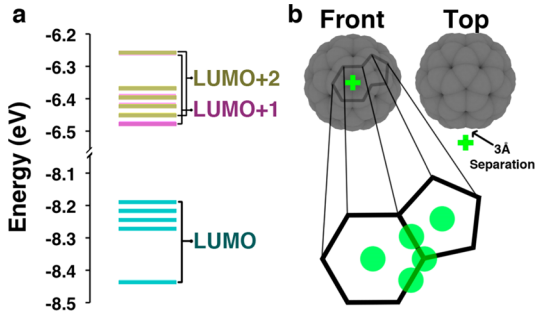

Figure 9. A nearby hole breaks the degeneracy of C_{60} LUMOs. If the broken symmetry in functionalized fullerenes were critical for bypassing the CT_0 state, the efficacy of C_{60} in vapor deposited devices would be inexplicable. Indeed, the critical orbital splitting is not actually a property of functionalization, but rather a property of the spherical fullerene unit. The unoccupied fullerene orbitals spatially occupy bands about each canonical Cartesian axis. When a point charge is nearby, one of these orbitals is always stabilized more greatly than the other two. (a) B3LYP/6-311++G** Kohn–Sham orbitals for seven placements (b) of an unscreened positive charge near a fullerene.

The existence of a resonant channel for dissociation contributed by the fullerene component implies a fundamental asymmetry in the role of donor and acceptor in promoting charge generation. In our study, this manifests itself in reduced charge transfer rates and increased geminate losses as the fullerene content of several blends is reduced.[12] Recent experiments have revealed additional properties asymmetrically promoted by donor and acceptor. Gélinas et al. showed that ultrafast charge separation from the heterojunction (<1 ps) is promoted by excess fullerene but reduced by excess donor.[11] Bernardo et al. also recently found that the delocalization of CT states is promoted by excess fullerene near the heterojunction but is unaffected by excess donor.[37]

The explanatory power of a "hot" channel for exciton dissociation, that bypasses bound, low-energy CT states is substantial: (i) bypassing bound intermediates explains the temperature and electric field independence of the early dynamics; (ii) the existence of a hot channel explains the general absence of Marcus inverted behavior in the charge transfer dynamics of working polymer/fullerene blends; (iii) the hot channel should be accessible from both relaxed and unrelaxed charge precursors, which is consistent with observations of equally efficient charge generation from donor and acceptor excitons and equally efficient diffusion-limited and prompt photogeneration; (iv) the contribution of the hot channel by the fullerene component explains the generality of these features across the great majority of studied devices.

Plausible alternate theories for efficient charge generation exist. Caruso and Troisi recently suggested that long-range dissociation may occur before nearest-neighbor transfer at the heterojunction.[38] Mechanistically, this is a form of "hot" transfer that also explains the above observations. The plausibility of this mechanism will ultimately depend on the accuracy of the long-range couplings that the model presupposes and the details of mapping this mechanism onto the actual blend quantum states. It has also been suggested that CT states are not, in fact, bound.[13] This would likewise explain the temperature and electric field independence of the early dynamics but needs to be reconciled with the substantial bimolecular recombination losses that mark most devices and myriad observations of geminate recombination.[7] For example, even blends that are highly efficient at generating free charge are typically <100 nm thick to avoid bimolecular recombination losses, which presupposes the reliable reformation of CT states but contradicts the idea of an unbound CT manifold. One possible explanation could be that a small number of recombination sites are responsible for most of the recombination observed in devices.

dx.doi.org/10.1021/ar5000852 | Acc. Chem. Res. 2014, 47, 3385–3394

CONCLUDING REMARKS

The mechanistic features of charge generation in both pristine and blended films of organic semiconductors are critically affected by the mesoscopic, many-molecule features of electronic structure. We have demonstrated here how DFT calculations can be used to build models of the charge generation process and can be scaled for mesoscopic calculations of cluster properties. Our ongoing work focuses on details of secondary charge separation from the heterojunction and the source of irreversibility during the charge generation process. Full elucidation of these details ultimately awaits accurate and scalable electronic structure calculations including hundreds of molecules—a goal not far off.

ASSOCIATED CONTENT

Supporting Information

Extended bibliography, electronic coupling methodological details, visualization of P3MT dimer and PTB7 dimer configurations paired with $PC_{60}BM$, C_{60} with proximate charge calculations, and oligomer length calculations. This material is available free of charge via the Internet at http://pubs.acs.org.

AUTHOR INFORMATION

Notes

The authors declare no competing financial interest.

Biographies

Brett M. Savoie earned B.S. degrees in chemistry and physics from Texas A&M University in 2008. He currently studies electronic processes in soft materials under the preceptorship of Mark Ratner and Tobin Marks. He drinks too much coffee but doesn't eat enough candy.

Nicholas E. Jackson received his B.A. in physics from Wesleyan University (Middletown, CT) in 2011 and is currently a Ph.D. candidate studying the mesoscopic conformational and electronic structure of conjugated polymers under the preceptorship of Mark Ratner and Lin Chen.

Lin X. Chen is a Senior Scientist in Argonne National Laboratory, a Professor of Chemistry in Northwestern University, and an AAAS Fellow. She received her B.Sc. from Peking University and Ph.D. from the University of Chicago, and postdoctoral training in the University of California at Berkeley. Her research interests are shown at http://chemgroups.northwestern.edu/chen_group/.

Tobin J. Marks is Vladimir Ipatieff Professor of Catalytic Chemistry and Professor of Materials Science and Engineering at Northwestern University. He received a B.S. degree from the University of Maryland and a Ph.D. degree from MIT. His research interests include the design, synthesis, characterization, and understanding of new functional electronic, photonic, and catalytic materials.

Mark A. Ratner obtained his B.A. and Ph.D. at Harvard and Northwestern Universities, respectively, and is Professor of chemistry and of materials science and engineering at Northwestern. He is interested in structure and function at the nanoscale and the theory of fundamental chemical processes. He spends as much time trout fishing as he possibly can.

ACKNOWLEDGMENTS

B.M.S. thanks Simon Gélinas for insightful comments during the writing of this manuscript. This work was supported as part of the ANSER Center, an Energy Frontier Research Center funded by the U.S. Department of Energy, Office of Science, Office of Basic Energy Sciences, under Award Number DE-SC0001059. N.E.J. thanks the NSF for a graduate research fellowship, and B.M.S. thanks the Northwestern MRSEC (NSF DMR-1121262) for a graduate research fellowship.

REFERENCES

(1) Würfel, P. *Physics of Solar Cells. From Principles to New Concepts*; Wiley: Weinheim, Germany, 2005.
(2) Shockley, W.; Queisser, H. Detailed Balance Limit of Efficiency of p-n Junction Solar Cells. *J. Appl. Phys.* **1961**, *32*, 510−519.
(3) Kearns, D.; Calvin, M. Photovoltaic Effect and Photoconductivity in Laminated Organic Systems. *J. Chem. Phys.* **1958**, *29*, 950.
(4) Tang, C. Two-Layer Organic Photovoltaic Cell. *Appl. Phys. Lett.* **1986**, *48*, 183−185.
(5) Yu, G.; Gao, J.; Hummelen, J.; Wudl, F.; Heeger, A. Polymer Photovoltaic Cells: Enhanced Efficiencies via a Network of Internal Donor-Acceptor Heterojunctions. *Science* **1995**, *270*, 1789−1791.
(6) Havinga, E. E.; Hoeve, W.; Wynberg, H. Alternate Donor-Acceptor Small-Band-Gap Semiconducting Polymers: Polyquaraines and Polycroconaines. *Synth. Met.* **1993**, *55*, 299−306.
(7) Bakulin, A. A.; Rao, A.; Pavelyev, V. G.; Van Loosdrecht, P. H. M.; Pshenichnikov, M. S.; Niedzialek, D.; Cornil, J.; Beljonne, D.; Friend, R. H. The Role of Driving Energy and Delocalized States for Charge Separation in Organic Semiconductors. *Science* **2012**, *335*, 1340−1344.
(8) Jailaubekov, A. E.; Willard, A. P.; Tritsch, J. R.; Chan, W.-L.; Sai, N.; Gearba, R.; Kaake, L. G.; Williams, K. J.; Leung, K.; Rossky, P. J.; Zhu, X.-Y. Hot Charge-Transfer Excitons Set the Time Limit for Charge Separation at Donor/Acceptor Interfaces in Organic Photovoltaics. *Nat. Mater.* **2013**, *12*, 66−73.
(9) Pensack, R.; Asbury, J. Barrierless Free Carrier Formation in an Organic Photovoltaic Material Measured with Ultrafast Vibrational Spectroscopy. *J. Am. Chem. Soc.* **2009**, *131*, 15986−15987.
(10) Kaake, L. G.; Moses, D.; Heeger, A. J. Coherence and Uncertainty in Nanostructured Organic Photovoltaics. *J. Phys. Chem. Lett.* **2013**, *4*, 2264−2268.
(11) Gelinas, S.; Rao, A.; Kumar, A.; Smith, S. L.; Chin, A. W.; Clark, J.; Van Der Poll, T. S.; Bazan, G. C.; Friend, R. H. Ultrafast Long-Range Charge Separation in Organic Semiconductor Photovoltaic Diodes. *Science* **2014**, *343*, 512−516.
(12) Savoie, B. M.; Rao, A.; Bakulin, A. A.; Gelinas, S.; Movaghar, B.; Friend, R. H.; Marks, T. J.; Ratner, M. A. Unequal Partnership: Asymmetric Roles of Polymeric Donor and Fullerene Acceptor in Generating Free Charge. *J. Am. Chem. Soc.* **2014**, *136*, 2876−2884.
(13) Vandewal, K.; Albrecht, S.; Hoke, E. T.; Graham, K. R.; Widmer, J.; Douglas, J. D.; Schubert, M.; Mateker, W. R.; Bloking, J. T.; Burkhard, G. F.; Sellinger, A.; Fréchet, J. M. J.; Amassian, A.; Riede, M. K.; Mcgehee, M. D.; Neher, D.; Salleo, A. Efficient Charge Generation by Relaxed Charge-Transfer States at Organic Interfaces. *Nat. Mater.* **2013**, *12*, 1−6.
(14) Shuttle, C.; O'Regan, B.; Ballantyne, A.; Nelson, J.; Bradley, D.; Durrant, J. Bimolecular Recombination Losses in Polythiophene: Fullerene Solar Cells. *Phys. Rev. B* **2008**, *78*, No. 113201.
(15) Savoie, B.; Movaghar, B.; Marks, T. J.; Ratner, M. A. Simple Analytic Description of Collection Efficiency in Organic Photovoltaics. *J. Phys. Chem. Lett.* **2013**, *4*, 704−709.
(16) Darancet, P.; Kronik, L.; Neaton, J. Low-Energy Charge-Transfer Excitons in Organic Solids from First-Principles: The Case of Pentacene. *J. Phys. Chem. Lett.* **2013**, *4*, 2197−2201.
(17) Sheng, C.; Tong, M.; Singh, S.; Vardeny, Z. Experimental Determination of the Charge/Neutral Branching Ratio η in the Photoexcitation of π-Conjugated Polymers by Broadband Ultrafast Spectroscopy. *Phys. Rev. B* **2007**, *75*, No. 085206.
(18) Savoie, B. M.; Jackson, N. E.; Marks, T. J.; Ratner, M. A. Reassessing the Use of One-Electron Energetics in the Design and Characterization of Organic Photovoltaics. *Phys. Chem. Chem. Phys.* **2013**, *15*, 4538−4547.
(19) Jackson, N. E.; Savoie, B. M.; Kohlstedt, K.; Cruz, O.; Schatz, G. C.; Marks, T. J.; Chen, L. X.; Ratner, M. A. Structural and

Conformational Dispersion in the Rational Design of Conjugated Polymers. *Macromolecules* **2014**, *47*, 987−992.
(20) Spano, F. The Spectral Signatures of Frenkel Polarons in H-and J-Aggregates. *Acc. Chem. Res.* **2009**, *43*, 429−439.
(21) Heitzer, H.; Marks, T.; Ratner, M. First-Principles Calculation of Dielectric Response in Molecule-Based Materials. *J. Am. Chem. Soc.* **2013**, *135*, 9753−9759.
(22) Onida, G.; Reining, L.; Rubio, A. Electronic Excitations: Density-Functional versus Many-Body Green's-Function Approaches. *Rev. Mod. Phys.* **2002**, *74*, 601−662.
(23) Tretiak, S.; Igumenshchev, K.; Chernyak, V. Exciton Sizes of Conducting Polymers Predicted by Time-Dependent Density Functional Theory. *Phys. Rev. B* **2005**, *41*, No. 033201.
(24) Kronik, L.; Stein, T.; Refaely-Abramson, S.; Baer, R. Excitation Gaps of Finite-Sized Systems from Optimally-Tuned Range-Separated Hybrid Functionals. *J. Chem. Theory Comput.* **2012**, *8*, 1515−1531.
(25) Chai, J. D.; Head-Gordon, M. Systematic Optimization of Long-Range Corrected Hybrid Density Functionals. *J. Chem. Phys.* **2008**, *128*, No. 084106.
(26) Tautz, R.; Da Como, E.; Limmer, T.; Feldmann, J.; Egelhaaf, H.-J.; Von Hauff, E.; Lemaur, V.; Beljonne, D.; Yilmaz, S.; Dumsch, I.; Allard, S.; Scherf, U. Structural Correlations in the Generation of Polaron Pairs in Low-Bandgap Polymers for Photovoltaics. *Nat. Commun.* **2012**, *3*, No. 970.
(27) Reid, O. G.; Pensack, R. D.; Song, Y.; Scholes, G.; Rumbles, G. Charge Photogeneration in Neat Conjugated Polymers. *Chem. Mater.* **2014**, *26*, 561−575.
(28) Szarko, J.; Rolczynski, B.; Lou, S.; Xu, T.; Strzalka, J.; Marks, T. J.; Yu, L.; Chen, L. X. Photovoltaic Function and Exciton/Charge Transfer Dynamics in a Highly Efficient Semiconducting Copolymer. *Adv. Funct. Mater.* **2014**, *24*, 10−26.
(29) Knupfer, M. Exciton Binding Energies in Organic Semiconductors. *Appl. Phys. A: Mater. Sci. Process.* **2003**, *77*, 623−626.
(30) Gélinas, S.; Kirkpatrick, J.; Howard, I.; Johnson, K.; Wilson, M. W. B.; Pace, G.; Friend, R. H.; Silva, C. Recombination Dynamics of Charge Pairs in a Push−Pull Polyfluorene-Derivative. *J. Phys. Chem. B* **2013**, *117*, 4649−4653.
(31) Liang, Z.; Gregg, B. A. Compensating Poly(3-hexylthiophene) Reveals Its Doping Density and Its Strong Exciton Quenching by Free Carriers. *Adv. Mater.* **2012**, *24*, 3258−3262.
(32) Park, S. H.; Roy, A.; Beaupré, S.; Cho, S.; Coates, N.; Moon, J. S.; Moses, D.; Leclerc, M.; Lee, K.; Heeger, A. J. Bulk Heterojunction Solar Cells with Internal Quantum Efficiency Approaching 100%. *Nat. Photonics* **2009**, *3*, 297−302.
(33) Schilinsky, P.; Waldauf, C.; Brabec, C. J. Recombination and Loss Analysis in Polythiophene Based Bulk Heterojunction Photodetectors. *Appl. Phys. Lett.* **2002**, *81*, 3885−3887.
(34) Bakulin, A. A.; Dimitrov, S. D.; Rao, A.; Chow, P. C. Y.; Nielsen, C. B.; Schroeder, B. C.; McCulloch, I.; Bakker, H. J.; Durrant, J. R.; Friend, R. H. Charge-Transfer State Dynamics Following Hole and Electron Transfer in Organic Photovoltaic Devices. *J. Phys. Chem. Lett.* **2013**, *4*, 209−215.
(35) Heitzer, H.; Savoie, B.; Marks, T. J.; Ratner, M. A. Organic Photovoltaics: Elucidating the Ultra-Fast Exciton Dissociation Mechanism in Disordered Materials. *Angew. Chem., Int. Ed.* **2014**, *53*, 1−6.
(36) Liu, T.; Troisi, A. What Makes Fullerene Acceptors Special as Electron Acceptors in Organic Solar Cells and How to Replace Them. *Adv. Mater.* **2013**, *25*, 1038−1041.
(37) Bernardo, B.; Cheyns, D.; Verreet, B.; Schaller, R. D.; Rand, B. P.; Giebink, N. C. Delocalization and Dielectric Screening of Charge Transfer States in Organic Photovoltaic Cells. *Nat. Commun.* **2014**, *5*, No. 3245.
(38) Caruso, D.; Troisi, A. Long-Range Exciton Dissociation in Organic Solar Cells. *Proc. Natl. Acad. Sci. U.S.A.* **2012**, *109*, 13498−13502.